3-Phenyl-5-(2-pyridyl)pyrazolato Complexes of Lithium, Magnesium, Calcium, and Zinc

Tobias Kloubert, Helmar Görls and Matthias Westerhausen

Institute of Inorganic and Analytical Chemistry, Friedrich Schiller University Jena, Humboldtstrasse 8, D-07743 Jena, Germany

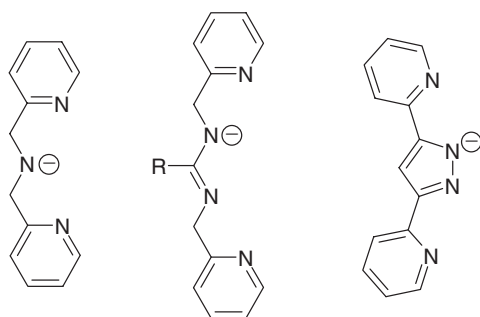Reprint requests to Prof. M. Westerhausen. E-mail: m.we@uni-jena.de

Dedicated to Professor Wolfgang Beck on the occasion of his 80th birthday

Metalation of 3-phenyl-5-(2-pyridyl)pyrazole (HPz, **1**) with alkyllithium and -zinc compounds in tetrahydrofuran (thf) yields dinuclear products [(thf)Li(Pz)]$_2$ (**2**) and [MeZn(Pz)]$_2$ (**3**), respectively. Magnesiation of **1** with diethylmagnesium in tetrahydrofuran in the presence of 1,4-dioxane leads to cocrystallization of mononuclear [(thf)$_2$Mg(Pz)$_2$] (**4a**) and [(diox)$_2$Mg(Pz)$_2$] (**4b**). Metalation of **1** with KH followed by a metathesis reaction with CaI$_2$ in tetrahydrofuran leads to the formation of dinuclear [{(thf)$_2$Ca}(μ-Pz)$_3$Ca(Pz)] (**5**) with the calcium atoms in different coordination environments. The ligand precursor **1** crystallizes as a dimer with N–H···N bridges between the pyrazole fragments. The pyrazolate anions of the metal complexes **2** to **5** exhibit similar structural parameters regardless of a bridging or terminal coordination mode and the electronegativity of the coordinated metal.

Key words: Calcium, Lithium, Magnesium, Metalation Reactions, Pyrazolates, Zinc
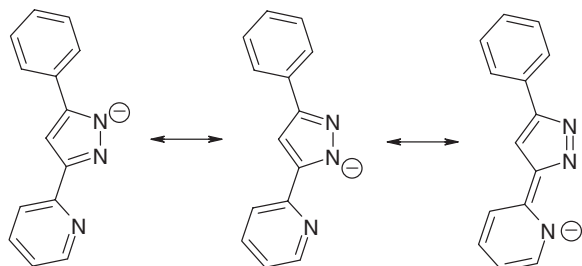
Introduction

In dinuclear metal complexes with multidentate aza ligands the non-bonding metal-metal distance plays a significant role regarding the reactivity in stoichiometric and catalytic reactions. In order to vary the intramolecular metal-metal contact, slight variations within the ligand backbone can induce a large influence. In Scheme 1 the principle is demonstrated restricting this concept to singly charged anions with outer 2-pyridyl substituents. For many of those anionic ligands diverse metal complexes have been studied extensively, probably the most important group being the bis(2-pyridylmethyl)amidinates of main group and transition metals [1]. Pyrazolates represent another class of ligands with extended applications [2 – 8].

A common problem in the chemistry of 3,5-bis(2-pyridyl)pyrazolato complexes is their low solubility in common organic solvents. Therefore, we investigated selected coordination compounds with 3-phenyl-5-(2-pyridyl)pyrazolato ligands (Pz) thus reducing the denticity of this ligand. In principle, three mesomeric forms can be formulated as shown in Scheme 2. The degree of contribution of the third formula influences the rotation barrier around the C–C bond. Computational investigations on a free 3-phenyl-5-(2-pyridyl)pyrazolate anion have shown that the charge is mainly localized on the pyrazolate moiety and that the rotation barrier shows a value of approximately 42 kJ mol^{-1} slightly depending on the solvent. In addition, the *trans* conformer is slightly favored by 7 (in tetrahydrofuran) up to 21 kJ mol^{-1} (for the free

Scheme 1. Examples of singly charged aza ligands with outer 2-pyridyl groups; bis(2-pyridylmethyl)amides (left), *N*,*N'*-bis(2-pyridylmethyl)amidinates (middle), 3,5-bis(2-pyridyl)pyrazolates (right).

Scheme 2. Mesomeric forms of the *cis* conformer of the 3-phenyl-5-(2-pyridyl)pyrazolate anion (Pz); the negative charge can formally be located on any nitrogen atom.

molecule) compared to the *cis* isomer which is shown in Scheme 2 [9].

AM1 calculations on 3-phenyl-5-(2-pyridyl)pyrazole (HPz, **1**), however, showed a preference of the *cis* conformer by 13.6 kJ mol^{-1} due to the hydrogen bridge between the pyridyl and the pyrazole fragments [10]. The formation of an N–H bond at the pyridyl group is higher in energy by 57.4 kJ mol^{-1} supporting that the break-up of the aromaticity of the pyridyl moiety is strongly disfavored. For the 1,2-migration of the proton from N1 to N2 at the pyrazole ring an energy of 13.4 kJ mol^{-1} has to be invested.

The interest in these 3-phenyl-5-(2-pyridyl)pyrazole and -pyrazolato ligands is founded on their rich coordination chemistry with metals of different sizes and oxidation states with the main focus on late transition metals such as cobalt [11, 12], nickel [12, 13], and copper [12, 14] as well as molybdenum [10], ruthenium [15, 16], palladium [17 – 19], and platinum [19, 20]. Recently, the coordination behavior of the extended ligand 2,6-bis(5-phenyl-1H-pyrazol-3-yl)pyridine towards d^{10} metal cations was also investigated [21]. The regioselective *N*-alkylation of the pyrazole ring succeeded *via* metalation with NaH or NaOEt with a subsequent metathesis reaction with alkyl halides [9]. Results of computational studies support the formation of a sodium complex with a bidentate pyrazolato ligand enforcing regioselective alkylation. Here, we add detailed studies of the coordination behavior of 3-phenyl-5-(2-pyridyl)pyrazolate anions towards the *s*-block metal ions of lithium, magnesium, and calcium as well as methylzinc cations.

Results and Discussion

Synthesis. 3-Phenyl-5-(2-pyridyl)pyrazole (HPz, **1**) was prepared according to a well-known protocol from 2-pyridinoyl-benzoylmethane and hydrazine hydrate [22]. For comparison with related compounds, its crystal structure was determined. The results verified the predicted molecular structure with an intramolecular N–H···N hydrogen bond stabilizing the *cis* conformer. Molecular structure and numbering scheme of
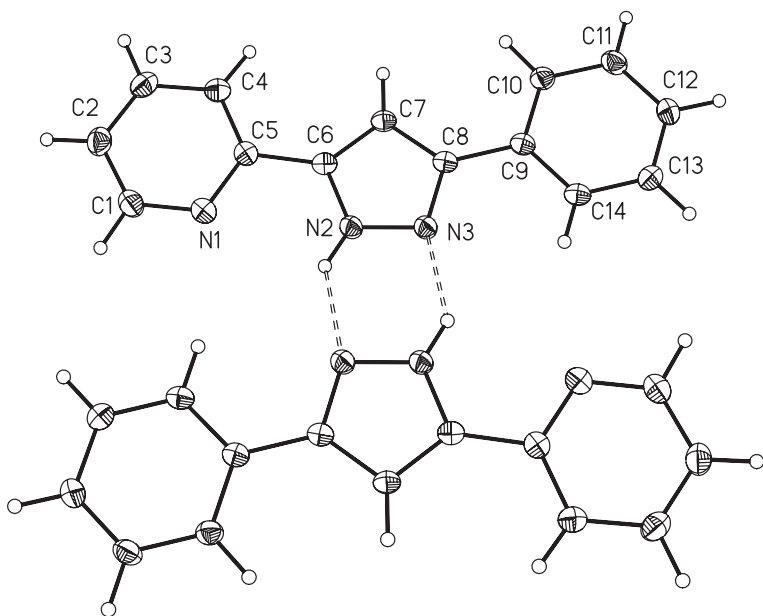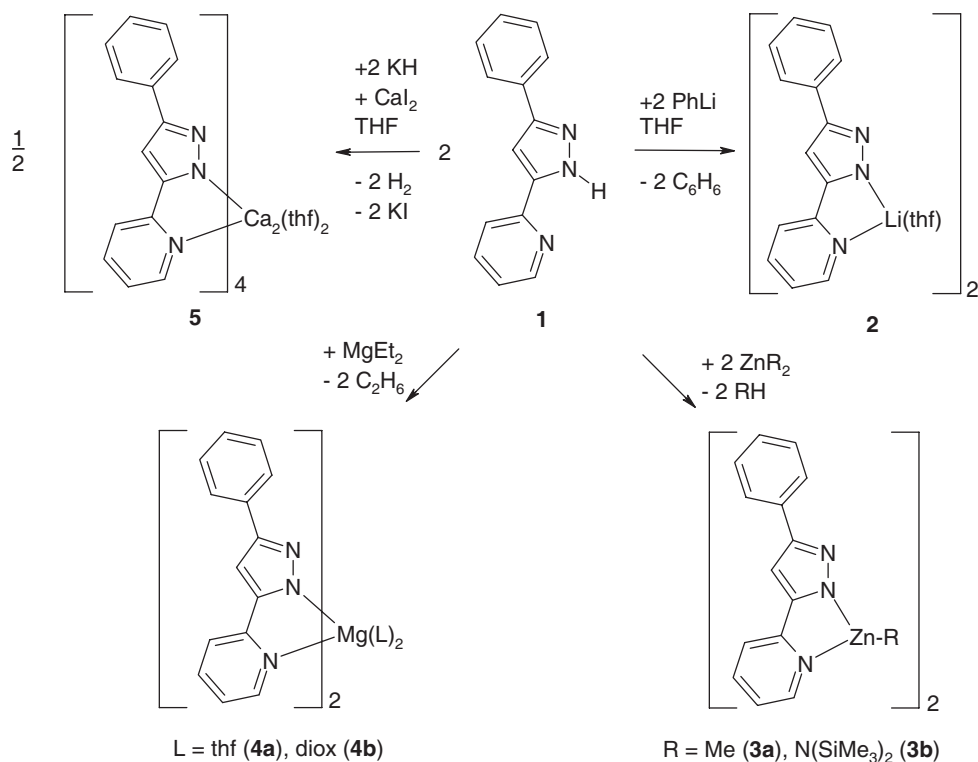

Fig. 1. Molecular structure and numbering scheme of 3-phenyl-5-(2-pyridyl)pyrazole (HPz, **1**). The ellipsoids represent a probability of 40%, H atoms are drawn with arbitrary radii. Selected bond lengths (pm): N2–N3 135.1(2), N2–C6 135.3(2), C6–C7 138.2(2), C7–C8 140.8(2), N3–C8 134.4(2), C5–C6 146.6(2), C8–C9 147.4(2).

Scheme 3. Metalation of 3-phenyl-5-(2-pyridyl)pyrazole (**1**) with phenyllithium, dimethylzinc, bis[bis(trimethylsilyl)amido]zinc, and diethylmagnesium yielding the corresponding complexes **2** to **4**; metalation of **1** with potassium hydride and subsequent metathesis reaction with calcium(II) iodide lead to the formation of dinuclear **5**.

1 are displayed in Fig. 1. The numbering scheme of the ligand is identical throughout all structure presentations. All hydrogen atoms were refined isotropically and the pyrazole hydrogen atom shown to be bound at N2 (N2–H 93(2) pm). Despite the localization of the *N*-bound hydrogen atom there exists a far-reaching delocalization of charge within the pyrazole ring. The N2–C6 and N3–C8 bond lengths are very similar and the same is true for the C6–C7 and C7–C8 bonds. This fact is understandable because the dimerization *via* N2–H···N3A hydrogen bridges decreases the difference between the chemical environments of N2 and N3. Despite the planarity of the molecule, the C–C bond lengths to the pyridyl (C5–C6 146.6(2) pm) and to the phenyl groups (C8–C9 147.4(2) pm) show no double bond character and represent values for single bonds between formally sp^2-hybridized carbon atoms.

In general, pyrazoles are quite acidic and, hence, easily deprotonated because pyrazolate anions are stabilized by five-membered aromatic ring systems.

Phenyllithium, dimethylzinc (Scheme 3, coordinated solvent is omitted), and diethylmagnesium were applied to metalate 3-phenyl-5-(2-pyridyl)pyrazole (**1**) because the alkane by-products are easily removed. Diethylmagnesium reacted with two equivalents of the pyrazole in thf in the presence of 1,4-dioxane (diox) according to Scheme 3 yielding mononuclear [(thf)$_2$Mg(Pz)$_2$] (**4a**) and [(diox)$_2$Mg(Pz)$_2$] (**4b**) which co-crystallized in equimolar amounts. In contrast to diethylmagnesium, dimethylzinc and bis[bis(trimethylsilyl)amido]zinc reacted only with equimolar amounts of 3-phenyl-5-(2-pyridyl)pyrazole regardless of the applied stoichiometry. Lithium and zinc derivatives crystallized as the dinuclear complexes [(thf)Li(Pz)]$_2$ (**2**), [MeZn(Pz)]$_2$ (**3a**) and [(Me$_3$Si)$_2$NZn(Pz)]$_2$ (**3b**).

Due to the fact that simple dialkylcalcium derivatives are unknown or challenging to prepare we reacted the pyrazole with potassium hydride and subsequently with calcium(II) iodide to give the dinuclear

$[\{(thf)_2Ca\}(\mu\text{-}Pz)_3Ca(Pz)]$ (**5**). The environments of the calcium atoms are different, and a rather complex structure was suggested by the broadened NMR resonances which showed no temperature-dependent sharpening or splitting into several signals.

In summary, we synthesized two complexes with a metal–pyrazolate ratio of 1 : 1 and two alkaline earth metal derivatives with a metal/pyrazolate ratio of 1 : 2. In order to obtain single crystals of good quality, 1,4-dioxane was added to the tetrahydrofuran solutions of the compounds. The magnesium complexes **4a**,**b** precipitated as monomeric molecules with hexacoordinate metal centers; thf or 1,4-dioxane molecules saturate the coordination sphere of this alkaline earth metal atom and are in *trans* position to each other. The calcium derivative **5** crystallized as a dimer with two ligands, however, the molecular structure proved to be rather complex containing alkaline earth metal atoms with different coordination numbers and chemical environments.

In order to discuss the coordination chemistry toward *s*-block metal atoms and the methylzinc cation X-ray structure determinations were performed.

Molecular structures

The molecular structure and numbering scheme of (tetrahydrofuran)lithium 3-phenyl-5-(2-pyridyl)pyrazolate ($[(thf)Li(Pz)]_2$, **2**) are displayed in Fig. 2. Molecular C_2 symmetry is destroyed by the orientation of the thf ligands. The ligands are chelating one

lithium cation and also bridging two such cations. This bridging leads to the formation of a six-membered Li_2N_4 ring with a trans-annular *cis* arrangement of the thf ligands. Whereas the Li–O bond lengths resemble characteristic values (av. 195.3 pm), the Li–N bond lengths vary within a large range. Due to electrostatic attraction the Li–N bond lengths to the pyrazolate anion are much shorter (av. 200.2 pm) than the bonds to the pyridyl groups (av. 214.1 pm). A smaller value of 193.2(7) pm was observed for bis(thf)lithium 2,5-di(*tert*-butyl)pyrrolide with a three-coordinate lithium atom [23]. Lithium amides represent an extensively investigated class of compounds due to their enormous importance as nucleophiles in deprotonation and transamination reactions. Hence, several excellent review articles deal with their structural properties [24 – 29]. The Li–N bonds to the pyridyl bases in **2** lie within the expected range as observed also for picolylamido- and 8-quinolylamido-lithium complexes with five-membered LiN_2C_2 rings (see *e. g.* refs. [30 – 35]).

Zinc pyrazolate complexes play an important role in bioinorganic chemistry as models for zinc enzymes [36 – 38]. In these complexes, the pyrazolato ligand acts as a bridging ligand between two zinc cations. The basic structure of the zinc derivative $[MeZn(Pz)]_2$ (**3a**) is very similar to that of complex **2**. The methyl groups also show a trans-annular *cis* arrangement leading to molecular C_2 symmetry with bridging pyrazolate anions. The zinc atoms are embedded in a distorted tetrahedral environment with

Fig. 2. Molecular structure and numbering scheme of dinuclear $[(thf)Li(Pz)]_2$ (**2**). The ellipsoids represent a probability of 40 %, H atoms are omitted for clarity. The asymmetric unit contains two dimers but only one of these molecules is shown. Selected bond lengths (pm): Li1A–O1A 193.5(8), Li1A–N3A 199.9(9), Li1A–N1B 213.4(10), Li1A–N2B 202.1(10), Li1B–O1B 197.1(8), Li1B–N3B 198.0(9), Li1B–N1A 214.7(9), Li1B–N2A 200.8(8).
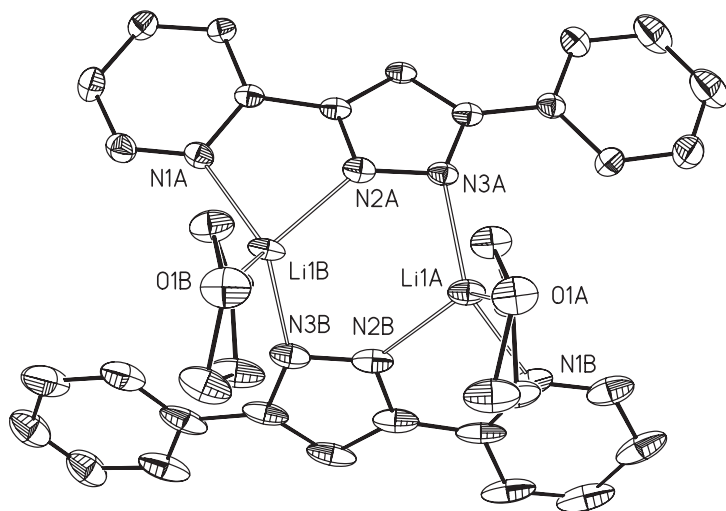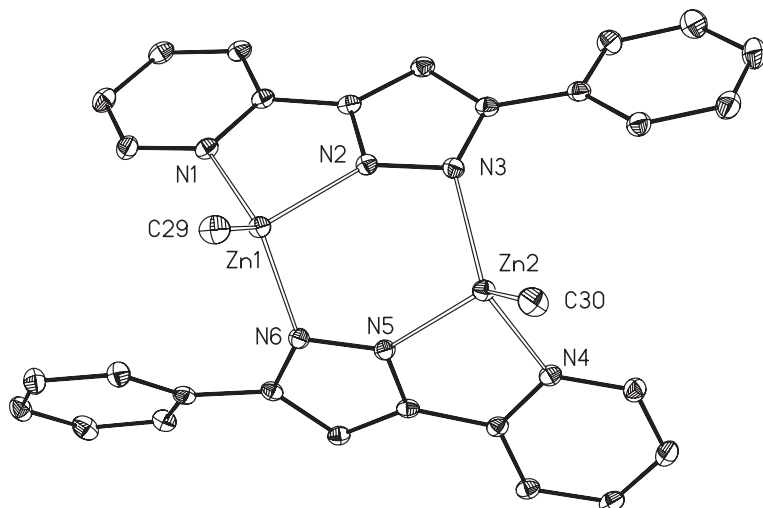
Fig. 3. Molecular structure and numbering scheme of [MeZn(Pz)]$_2$ (**3a**). The ellipsoids represent a probability of 40 %, H atoms are neglected. Selected bond lengths (pm): Zn1–C29 197.0(2), Zn1–N1 211.9(2), Zn1–N2 205.2(2), Zn1–N6 205.5(2), Zn2–C30 197.4(2), Zn2–N3 208.2(2), Zn2–N4 215.7(2), Zn2–N5 204.8(2).
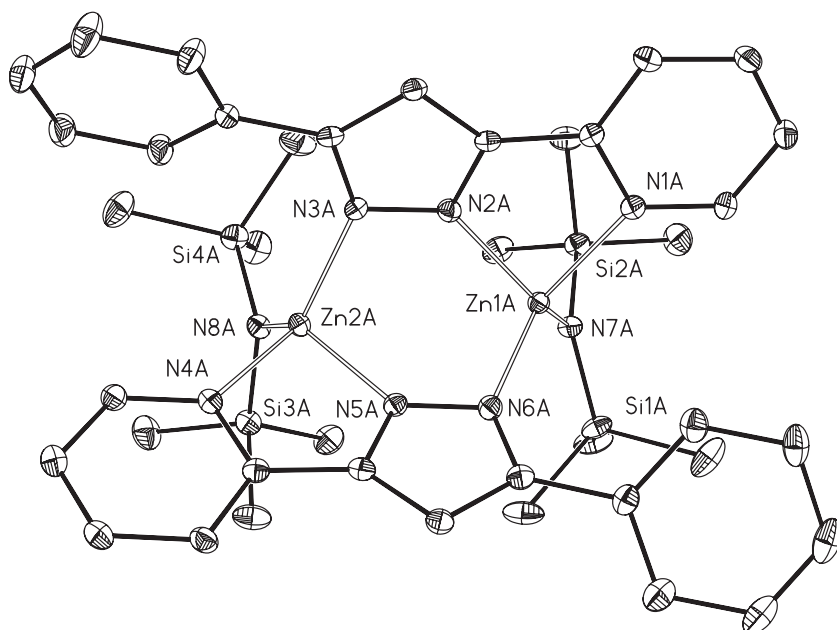

Fig. 4. Molecular structure and numbering scheme of [(Me$_3$Si)$_2$NZn(Pz)]$_2$ (**3b**). The ellipsoids represent a probability of 40 %, H atoms are omitted for clarity. The asymmetric unit contains two molecules A and B; only molecule A is shown. Selected bond lengths (pm) of molecule A (molecule B in square brackets): Zn1A–N7A 190.4(2) [191.5(2)], Zn1A–N1A 214.1(2) [212.8(2)], Zn1A–N2A 205.7(2) [207.6(2)], Zn1A–N6A 204.3(2) [203.6(2)], Zn2A–N8A 191.8(2) [190.5(2)], Zn2A–N3A 203.1(2) [203.9(2)], Zn2A–N4A 214.9(2) [212.1(2)], Zn2A–N5A 206.5(2) [206.3(2)].

the 3-phenyl-5-(2-pyridyl)pyrazolate anions acting as bidentate and bridging ligands. Molecular structure and numbering scheme of **3a** are shown in Fig. 3. The Zn–C bond lengths adopt values characteristic of tetra-coordinate zinc atoms [39]. Enhancement of steric strain by replacement of the zinc-bound methyl group by a bis(trimethylsilyl)amide anion (leading to structure **3b**) only leads to minor changes (Fig. 4). The structure is very similar, with trans-annular *cis*-arranged bis(trimethylsilyl)amido ligands

as observed for 3,5-di(2-pyridyl)pyrazolato-zinc bis(trimethylsilyl)amide [40]. Again, the metal-nitrogen distances to the pyrazolate anions are smaller than those to the pyridyl substitutents. Similar observations were already discussed in detail for picolylamido- as well as 8-quinolylamido-zinc derivatives (see for example refs. [41 – 47]).

The molecular structures and numbering schemes of [(thf)$_2$Mg(Pz)$_2$] (**4a**) and [(diox)$_2$Mg(Pz)$_2$] (**4b**) are represented in Fig. 5. In these mononuclear com-
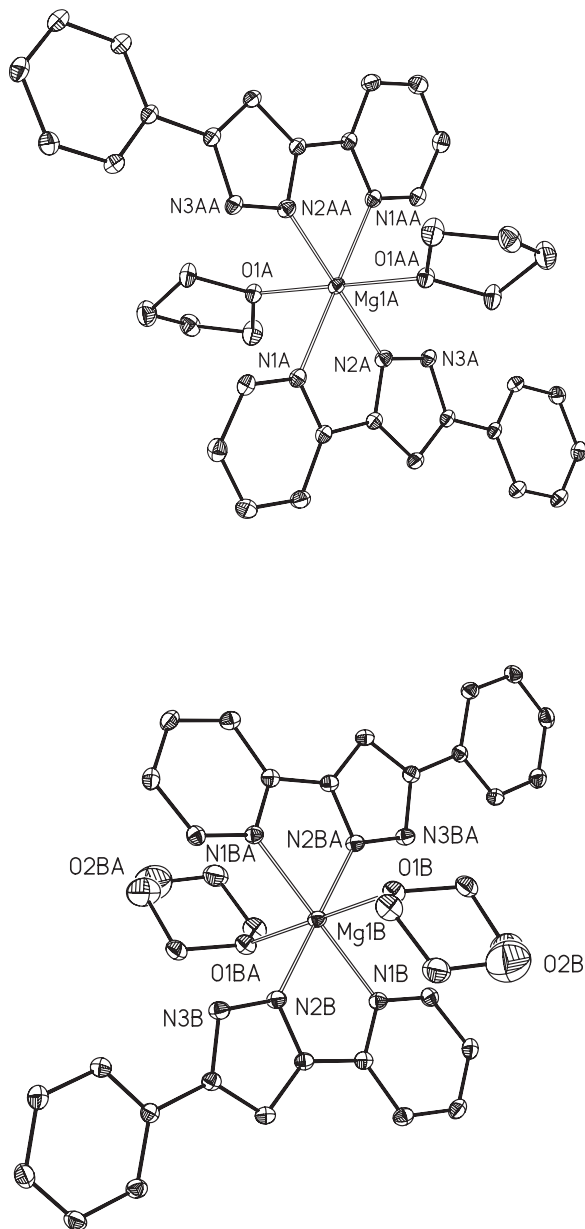
Fig. 5. Molecular structure and numbering scheme of mononuclear $[(thf)_2Mg(Pz)_2]$ (**4a**, top, molecule A) and $[(diox)_2Mg(Pz)_2]$ (**4b**, at the bottom, molecule B). The asymmetric units contain two half molecules that are completed by the symmetry operations $(-x, -y, -z)$ and $(-x+1, -y, -z+1)$ for molecules A and B, respectively. Selected bond lengths (pm): Mg1A–N1A 219.5(2), Mg1A–N2A 208.2(2), Mg1A–O1A 216.0(2), Mg1B–N1B 215.9(2), Mg1B–N2B 210.1(2), Mg1B–O1B 216.3(2).

plexes the magnesium atoms are bound to two bidentate 3-phenyl-5-(2-pyridyl)pyrazolate anions and to two ether ligands. The asymmetric unit contains two molecules which differ by their ether ligands: One complex contains two thf ligands, the other two 1,4-dioxane molecules in *trans* positions. The complexes have the metal atoms at the inversion centers. The Mg–N bonds to the pyridyl groups are longer than those

to the pyrazolate moieties. A similar behavior was also found for picolylamido- and 8-quinolylamido-magnesium derivatives [45 – 47].

The larger size of calcium and the enhanced ionic character lead to a unique dimerization in $[\{(thf)_2Ca\}(\mu\text{-Pz})_3Ca(Pz)]$ (**5**). The molecular structure and numbering scheme are shown in Fig. 6. The coordination spheres of the calcium atoms differ significantly. The six-coordinate atom Ca1 is in a distorted octahedral environment of two thf molecules in a *cis* arrangement and four nitrogen atoms of three pyrazolate anions and of one pyridyl group. The seven-coordinate atom Ca2 is surrounded by three bidentate pyridylpyrazolato units and an additional pyrazolato nitrogen atom. Thus, three pyrazolate anions act as bridging ligands whereas one anion binds as a terminal bidentate ligand to Ca2. The irregular coordination pattern leads to large variation of the Ca1–O (238.5(3) and 245.3(3) pm) and Ca–N bond lengths (238.7(3) to 264.6(3) pm). These restraints and the three bridging pyrazolato units allow for a rather short non-bonding Ca1···Ca2 contact of 367.1(1) pm. In tris(pyrazolyl)methanide complexes of calcium comparable Ca–N bond lengths were observed between neutral pyrazolyl units and five- as well as six-coordinate calcium centers [48]. Strong electrostatic attraction between calcium cations and amide anions leads to shorter Ca–N bond lengths [8, 49 – 55] supporting the importance of electrostatic interactions in mainly ionic amidocalcium complexes.

The 3-phenyl-5-(2-pyridyl)pyrazolate anions always act as bidentate ligands forming five-membered rings with the metal ions. Side-on coordination has already been observed when oligomerization of the complexes occurred, but this coordination behavior was restricted to the heaviest alkaline earth metals [8]. Aggregation with the lighter *s*-block metal atoms lithium and calcium as well as zinc was always encountered with
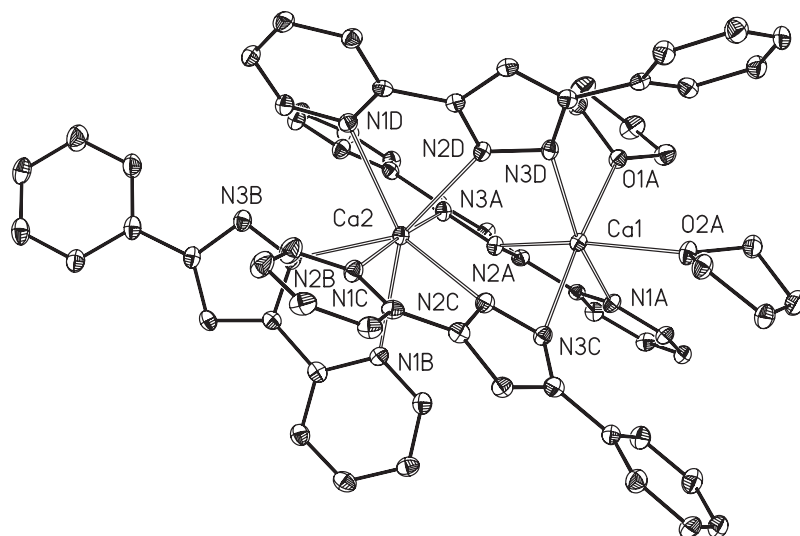
Fig. 6. Molecular structure of dinuclear $[\{(thf)_2Ca\}(\mu\text{-Pz})_3Ca(Pz)]$ (**5**). The ellipsoids represent a probability of 40%, H atoms are neglected for clarity. The pyrazolate anions are distinguished by the letters A, B, C, and D. Selected bond lengths (pm): Ca1–O1 245.3(3), Ca1–O2 238.5(3), Ca1–N1A 248.9(3), Ca1–N2A 245.1(3), Ca1–N3C 240.0(4), Ca1–N3D 238.7(3), Ca2–N3A 242.8(3), Ca2–N1B 263.2(3), Ca2–N2B 247.5(4), Ca2–N1C 250.0(3), Ca2–N2C 257.3(4), Ca2–N1D 264.6(3), Ca2–N2D 256.5(3).

Table 1. Selected structural data of 3-phenyl-5-(2-pyridyl)pyrazole (HPz, **1**) and the 3-phenyl-5-(2-pyridyl)pyrazolate anions of the lithium (**2**), zinc (**3a** and **3b**), magnesium (**4**), and calcium derivatives (**5**) (bond lengths in pm).

Compound	Ligand	N2–N3	N2–C6	N3–C8	C6–C7	C7–C8	C6–C5	C8–C9
HPz (**1**)		135.1(2)	135.3(2)	134.4(2)	138.2(2)	140.8(2)	146.6(2)	147.4(2)
[(thf)Li(Pz)]$_2$ (**2**)	A	136.3(5)	135.4(5)	136.5(5)	139.3(6)	140.1(6)	147.1(6)	145.2(7)
	B	136.5(7)	134.5(6)	135.5(6)	138.5(9)	140.8(9)	146.4(10)	144.8(9)
	C	136.1(6)	135.1(6)	135.6(6)	139.4(7)	138.4(7)	146.8(7)	148.4(7)
	D	135.5(5)	136.3(5)	135.4(5)	139.5(6)	139.9(6)	146.7(6)	147.5(6)
[MeZn(Pz)]$_2$ (**3a**)	A	135.3(2)	134.3(2)	136.2(2)	139.4(2)	139.5(3)	146.4(3)	146.9(3)
	B	135.3(2)	134.4(2)	135.3(2)	139.4(2)	140.0(3)	146.6(2)	147.1(2)
[(Me$_3$Si)$_2$NZn(Pz)]$_2$ (**3b**)	A	134.7(3)	135.3(3)	136.0(3)	139.9(4)	139.6(4)	145.5(4)	146.4(4)
	B	135.4(3)	134.6(4)	135.5(4)	139.6(4)	139.6(4)	146.3(4)	148.3(4)
	C	135.6(3)	134.9(4)	135.2(4)	139.2(4)	139.4(4)	146.1(4)	146.8(4)
	D	136.0(3)	134.5(3)	136.0(3)	139.6(4)	139.7(4)	145.8(4)	147.0(4)
[(thf)$_2$Mg(Pz)$_2$] (**4a**)	A	135.7(2)	136.1(3)	135.6(3)	139.7(3)	139.9(3)	146.0(3)	147.6(3)
[(diox)$_2$Mg(Pz)$_2$] (**4b**)	B	135.6(3)	135.9(3)	135.1(3)	139.2(3)	140.2(3)	146.1(3)	147.7(3)
[{(thf)$_2$Ca}(μ-Pz)$_3$Ca(Pz)] (**5**)	A	136.5(5)	136.3(5)	136.1(5)	138.9(6)	139.6(6)	146.9(6)	146.2(6)
	B	135.8(5)	136.8(5)	134.8(5)	139.1(6)	138.7(6)	145.4(6)	147.2(6)
	C	137.3(5)	135.8(5)	135.8(5)	139.1(6)	139.2(6)	146.4(6)	147.3(6)
	D	136.3(5)	135.4(5)	136.0(5)	139.4(6)	138.9(6)	146.1(6)	146.5(6)

bridging pyrazolate fragment. Selected bond lengths of the pyrazolate anions are listed in Table 1. It is surprising that these parameters neither depend on the charge and electronegativity of the metals nor on the terminal or bridging coordination mode. The charge appears to be completely delocalized within the pyrazolate moiety. The bonds between the pyrazolate unit and the pyridyl (C5–C6) and phenyl substituents (C8–C9) are rather short for C–C bonds between sp^2-hybridized carbon atoms suggesting a slight charge delocalization into the π systems of these groups. The planarity of the 3-phenyl-5-(2-pyridyl)pyrazolate anions supports the

extended charge delocalization. Obviously, the phenyl and pyridyl units express a similar electronic influence on the pyrazolate ring making the endocyclic N2–C6 and N3–C8 bond lengths equal within the standard deviations. These observations suggest that the bonding situation between the metal cations and the pyrazolate anions is mainly based on electrostatic contributions.

NMR studies

For determining electronic effects, NMR spectroscopy represents an excellent tool. However, due to

NMR	1	2	3a	3b	4	5
δ(H4)	7.17	6.94	6.84	6.87	7.05	7.07
δ(C31)	135.1	138.0	135.2	135.5	138.0	138.2
δ(C3)	143.8	152.9	154.7	154.9	154.4	151.9
δ(C4)	100.5	98.9	100.8	101.2	98.8	100.2
δ(C5)	149.7	151.9	148.2	149.1	149.7	151.9
δ(C51)	153.0	156.3	151.2	151.2	153.7	155.6

Table 2. Selected chemical shifts δ (ppm) of 3-phenyl-5-(2-pyridyl)pyrazole (HPz, **1**) and the 3-phenyl-5-(2-pyridyl)pyrazolate anions of the lithium (**2**), zinc (**3a** and **3b**), magnesium (**4**), and calcium derivatives (**5**).

the poor solubility of compounds **2**–**5** strong Lewis bases had to be added in order to obtain acceptable signal-to-noise ratios. Therefore, the molecular structures in the crystalline phase and in solution can be different, allowing for deaggregation, dissociation and exchange processes fast on the NMR time scale. This dynamic behavior leads to chemically equivalent anions and makes it impossible to distinguish between a terminal and a bridging coordination mode of the pyrazolato ligands. The ionicity of the bonding situation becomes obvious from the chemical ^{1}H and ^{13}C NMR shifts.

Selected NMR parameters are summarized in Table 2. The numbering scheme is shown in Scheme 4 and differs from the numbering used for the crystal structures. Expectedly, the ^{13}C{^{1}H} NMR resonance of C3 of **1** differs significantly from that of the deprotonated pyrazols. The chemical shifts of C4 and C5 show only very small differences. However, despite the fact that the influence of the metal on the chemical shifts is rather small, characteristic trends can be observed. Increasingly ionic bonding (*i. e.* decreasing electronegativity of the metal) leads to a low field shift of C5 and the *ipso*-carbon atom C51 of the pyridyl group. The NMR values of the lithium and the calcium derivatives are very similar due to comparable electronegativities even though the solid-state structures show no similarities. This observation can easily be explained assuming that planar anions and metal cations maximize electrostatic attraction and minimize inter-ligand

repulsion. Therefore the large calcium atom gives rise to large coordination numbers whereas lithium is generally four-coordinate.

Experimental

General: All manipulations were carried out in an argon or nitrogen atmosphere under anaerobic conditions. Prior to use, all solvents were thoroughly dried and distilled in an inert gas atmosphere. ^{1}H NMR and ^{13}C NMR spectra were recorded at ambient temperature on Bruker AC 200 MHz, AC 400 MHz or AC 600 MHz spectrometers. All spectra were referenced to the deuterated solvent as an internal standard. EI-mass spectra were obtained on a Finnigan MAT SSQ 710 system. Masses marked with an asterisk contain the appropriate metal atom according to the isotopic pattern. IR measurements were carried out on a Perkin Elmer System 2000 FT-IR. The values of the elemental analyses deviate from theoretical values because weighing of these moisture sensitive compounds was challenging due to the easy loss of co-crystallized thf and also due the carbonate formation during combustion even though V_2O_5 was added. Decomposition and melting points were measured with a Reichert-Jung apparatus Type 302102. 3-Phenyl-5-(2-pyridyl)pyrazole (HPz, **1**) was prepared according to a literature procedure [22].

*Synthesis of HPz (**1**)*

1-Phenyl-3-(2-pyridyl)propane-1,3-dione (22.5 g, 99.4 mmol) was dissolved in 150 mL of ethanol and heated under reflux. Hydrazine hydrate (10 g, 0.2 mol) was added dropwise. After 2 h the addition of hydrazine hydrate was repeated with the same amount, and reflux conditions were maintained for additional two h. Removal of all volatiles and recrystallization of the residue from toluene gave colorless needles of **1**. Yield: 17.3 g of crystalline **1** (78.2 mmol, 79 %). M. p. 168 °C. – ^{1}H NMR (400 MHz, 303 K, ([D$_8$]thf): δ = 12.7 (br. s, 1H, H[1]), 8.57 (d, ^3J(H[53],H[54]) = 4.8 Hz, 1H, H[53]), 7.86–7.84 (m, 3H, H[32,56]), 7.75 (t, ^3J(H[55],H[54,56]) = 7.6 Hz, 1H, H[55]), 7.37 (t, ^3J(H[33],H[32,34]) = 7.6 Hz, 2H, H[33]), 7.25 (t, ^3J(H[34],H[33]) = 7.5 Hz, 1H, H[34]), 7.21–7.17 (m, 1H, H[54]), 7.17 (s, 1H, H[4]). – ^{13}C NMR (600 MHz, 300 K, ([D$_8$]thf): δ = 153.0 (C[51]), 150.1 (C[53]), 149.7 (C[5]), 143.8 (C[3]), 137.4 (C[55]), 135.1 (C[31]), 129.0 (C[33]), 127.9
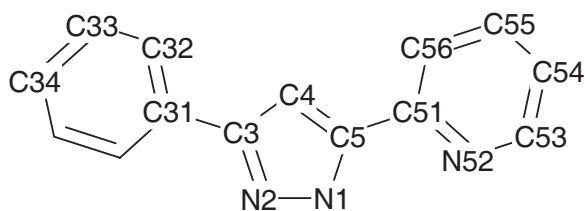
Scheme 4. Numbering scheme for the assignment of the ^{1}H and ^{13}C NMR spectra. The numbers of hydrogen atoms are identical to those of the attached carbon atoms.

(C^{34}), 126.0 (C^{32}), 123.0 (C^{54}), 120.3 (C^{56}), 100.5 (C^4). – MS (EI): m/z (%) = 221 (100) [M]$^+$, 192 (85) [M–N$_2$]$^+$, 165 (24), 115 (20), 78 (22) [C$_5$H$_4$N]$^+$. – IR (cm^{-1}): v = 3237 br.s, 3061 w, 3006 vw, 1597 m, 1585 m, 1469 s, 1449 vs, 1386 m, 1314 m, 1297 s, 1270 m, 1174 vs, 1148 m, 1076 vs, 995 vs, 971 vs, 957 vs, 912 m, 802 m, 780 s, 756 vs, 733 s, 719 s, 690 s, 682 s, 658 s, 620 s, 516 m, 508 s, 485 s, 419 w. – Elemental analysis for C$_{14}$H$_{11}$N$_3$, (221.26): calcd. C 76.00, H 5.01, N 18.99; found C 76.01, H 4.93, N 19.19.

Synthesis of [(thf)Li(Pz)]$_2$ (2)

2-(3-Phenyl-1H-pyrazol-5-yl)pyridine (778 mg, 3.52 mmol) was dissolved in 15 mL of thf. Phenyllithium (5.51 mL, c = 0.638 M, 3.52 mmol) was added dropwise, and a colorless precipitate of **2** formed quantitatively. In order to obtain single-crystalline material a small amount of the precipitate was dissolved in hot thf. Cooling led to the formation of colorless needles. M. p. 358 °C. – ^{1}H NMR (600 MHz, 300 K, [D$_8$]thf): δ = 8.59 (d, ^3J(H^{53},H^{54}) = 4.9 Hz, 1H, H^{53}), 7.95 (d, ^3J(H^{32},H^{33}) = 7.6 Hz, 2H, H^{32}), 7.74 (t, ^3J(H^{55},H^{33}) = 7.6 Hz, ^4J(H^{55},H^{53}) = 1.2 Hz, 1H, H^{55}), 7.66 (d, ^3J(H^{56},H^{55}) = 7.7 Hz, 1H, H^{56}), 7.35 (t, ^3J(H^{33},H^{32,34}) = 7.7 Hz, 2H, H^{33}), 7.14–7.12 (m, 2H, H^{34,54}), 6.94 (s, 1H, H^4). – ^{13}C NMR (600 MHz, 300 K, [D$_8$]thf): δ = 156.3 (C^{51}), 152.9 (C^3), 151.9 (C^5), 149.2 (C^{53}), 138.1 (C^{55}), 138.0 (C^{31}), 128.8 (C^{33}), 125.7 (C^{34}), 125.4 (C^{32}), 120.9 (C^{54}), 119.7 (C^{56}), 98.9 (C^4). – MS (EI): m/z (%) = 234 (52), 227* (100) [M–thf]$^+$. – IR (cm^{-1}): v = 3066 w, 3051 w, 3004 w, 2974 w, 2876 w, 1600 vs, 1593 m, 1527 s, 1455 s, 1441 vs, 1390 vw, 1332 w, 1230 m, 1178 m, 1152 m, 1106 m, 1075 s, 1051 s, 1006 m, 983 vs, 964 m, 909 m, 842 vw, 807 w, 783 s, 755 vs, 723 s, 687 vs, 679 vs, 633 s, 525 m, 484 vs, 439 m, 422 vs, 408 vs.

Synthesis of [MeZn(Pz)]$_2$ (3a)

2-(3-Phenyl-1H-pyrazol-5-yl)pyridine (**1**) (500 mg, 2.26 mmol) was dissolved in 30 mL of thf and cooled to –78 °C. Dimethylzinc (1.9 mL, c = 1.2 M, 2.28 mmol) was added dropwise. Then the reaction mixture was stirred over night and warmed to r. t. A colorless precipitate formed and was redissolved easily under heating. The product crystallized as colorless cubes. Yield: 675 mg of **3** (2.24 mmol, 99%). M. p. > 260 °C (dec.). – ^{1}H NMR (600 MHz, 300 K, [D$_8$]thf): δ = 7.81 (d, ^3J(H^{32},H^{33}) = 7.4 Hz, 2H, H^{32}), 7.73 (d, ^3J(H^{53},H^{54}) = 4.3 Hz, 1H, H^{53}), 7.55 (t, ^3J(H^{55},H^{56,54}) = 7.4 Hz, 1H, H^{55}), 7.47 (d, ^3J(H^{56},H^{55}) = 7.7 Hz, 1H, H^{56}), 7.16–7.13 (m, 1H, H^{34}), 7.10–7.08 (m, 2H, H^{33}), 6.94–6.92 (m, 1H, H^{54}), 6.84 (s, 1H, H^4), –0.61 (s, 1.5H, CH$_3$). – ^{13}C NMR (600 MHz, 300 K, [D$_8$]thf): δ = 154.7 (C^3), 151.2 (C^{51}), 148.6 (C^{53}), 148.2 (C^5), 138.2 (C^{55}), 135.2 (C^{31}), 128.9 (C^{33}), 127.7 (C^{32}), 127.2

(C^{34}), 122.5 (C^{54}), 119.2 (C^{56}), 100.8 (C^4), –11.5 (CH$_3$). – MS (EI): m/z (%) = 587* (38) [2M–CH$_3$]$^+$, 299* (48) [M]$^+$, 284* (44) [M–CH$_3$]$^+$, 192 (58) [M–ZnCH$_3$,N$_2$]$^+$, 94 (63), 79 (100) [C$_5$H$_5$N]$^+$. – IR (cm^{-1}): v = 2937 w, 2895 w, 2826 w, 1699 vw, 1607 vs, 1567 w, 1538 w, 1470 vs, 1447 vw, 1432 m, 1393 m, 1341 vw, 1286 m, 1258 w, 1235 m, 1204 m, 1152 m, 1125 m, 1083 m, 1064 m, 1016 s, 996 w, 968 w, 906 w, 884 m, 833 w, 798 s, 779 vs, 758 s, 727 m, 693 m, 638 vs, 522 vs, 492 m, 481 m, 463 m, 414 vs. – Elemental analysis for C$_{15}$H$_{13}$N$_3$Zn (300.66): calcd. C 59.92, H 4.36, N 13.98; found C 60.66, H 5.49, N 12.69.

Synthesis of [(Me$_3$Si)$_2$NZn(Pz)]$_2$ (3b)

2-(3-Phenyl-1H-pyrazol-5-yl)pyridine (**1**) (577 mg, 2.61 mmol) was dissolved in 20 mL of thf and cooled to 0 °C. Bis[bis(trimethylsilyl)amino]zinc (1 g, 2.60 mmol) was added dropwise and the reaction mixture stirred over night. The solvent was removed and the crude product recrystallized from toluene. Yield: 990 mg (2.22 mmol, 85%). M. p. 295 °C. – ^{1}H NMR (600 MHz, 300 K, [D$_8$]thf): δ = 8.35 (d, ^3J(H^{53},H^{53}) = 5.3 Hz, 1H, H^{53}), 7.98 (t, ^3J(H^{55},H^{56,54}) = 7.9 Hz, ^4J(H^{55},H^{53,}) = 1.6 Hz, 1H, H^{55}), 7.81 (d, ^3J(H^{56},H^{55}) = 7.9 Hz, 1H, H^{56}), 7.64 (d, ^3J(H^{32},H^{33}) = 7.8 Hz, 2H, H^{32}), 7.42–7.37 (m, 3H, H^{54,33}), 7.35–7.34 (m, 1H, H^{34}), 6.87 (s, 1H, H^4), –0.04 (s, 18H, SiMe$_3$). – ^{13}C NMR (600 MHz, 300 K, [D$_8$]thf): δ = 154.9 (C^3), 151.2 (C^{51}), 149.1 (C^5), 148.9 (C^{53}), 141.2 (C^{55}), 135.5 (C^{31}), 129.3 (C^{33}), 128.5 (C^{34}), 127.5 (C^{32}), 124.0 (C^{54}), 121.2 (C^{56}), 101.2 (C^4), 6.3 (SiMe$_3$). – MS (EI): m/z (%) = 505* (13) [M–N(SiMe$_3$)$_2$, 2 SiMe$_3$, C$_5$H$_5$N]$^+$, 221 (18) [ligand]$^+$, 146 (10) [(N(SiMe$_3$)$_2$)$_2$]$^+$, 130 (22) [(N(SiMe$_3$)$_2$)$_2$–MeH]$^+$. – IR (cm^{-1}): v = 3060 m, 2953 m, 2892 w, 1603 vs, 1570 m, 1539 w, 1517 w, 1472 m, 1447 vs, 1406 m, 1340 m, 1248 vs, 1181 m, 1151 m, 1124 m, 1083 w, 1050 w, 1012 s, 995 vs, 970 m, 927 vs, 884 m, 825 vs, 780 s, 755 vs, 727 vs, 694 vs, 634 m, 552 m, 494 m, 447 m, 432 w, 407 m. – Elemental analysis for C$_{20}$H$_{28}$N$_4$Si$_2$Zn (446.04): calcd. C 53.86, H 6.33, N 12.56; (+1/3 toluene: C 55.10, H 6.41, N 12.14); found C 55.30, H 6.66, N 11.63.

Synthesis of [(thf)$_2$Mg(Pz)$_2$] (4a) and [(diox)$_2$Mg(Pz)$_2$] (4b)

2-(3-Phenyl-1H-pyrazol-5-yl)pyridine (304 mg, 1.37 mmol) was dissolved in 15 mL of thf. Diethylmagnesium-1,4-dioxane (117 mg, 0.68 mmol), dissoved in 5 mL of thf, was added dropwise. Removal of 70% of the solvent, addition of 2 mL of 1,4-dioxane and storage at 4 °C produced colorless needles. Yield: 170 mg of a 1 : 1 mixture of **4a** and **4b** (0.53 mmol, 37%). M. p. 228 °C. – ^{1}H NMR (400 MHz, 300 K, [D$_8$]thf): δ = 8.23 (d, ^3J(H^{53},H^{54}) = 4.8 Hz, 1H, H^{53}), 8.01 (d, ^3J(H^{32},H$^{3'',33}$) = 7.5 Hz, 2H, H^{32}), 7.69 (t, ^3J(H^{55},H^{54,56}) = 7.8 Hz, ^4J(H^{55},H^{53,}) = 1.6 Hz, 1H, H^{55}), 7.62 (d, ^3J(H^{56},H^{55}) = 7.9 Hz, 1H, H^{56}),

Table 3. Crystal data and refinement details for the X-ray structure determinations of the compounds **1** to **5**.

Compound	1	2	3a	3b	4	5
Formula	$C_{14}H_{11}N_3$	$C_{36}H_{36}Li_2N_6O_2$, $^{1}/_{2}$ C_4H_8O	$C_{30}H_{26}N_6Zn_2$	$C_{40}H_{56}N_8Si_4Zn_2$	$C_{36}H_{36}MgN_6O_4$, $C_{36}H_{36}MgN_6O_2$	$C_{64}H_{56}Ca_2N_{12}O_2$, 3 C_4H_8O
Fw, g mol^{-1}	221.26	634.64	601.31	892.03	625.02	1321.68
T, °C	−140(2)	−140(2)	−140(2)	−140(2)	−140(2)	−140(2)
Crystal system	monoclinic	orthorhombic	monoclinic	triclinic	monoclinic	triclinic
Space group	$P2_1/n$	$P2_12_12_1$	$P2_1/n$	$P\bar{1}$	$P2_1/n$	$P\bar{1}$
a, Å	5.6263(2)	14.7350(2)	15.7752(2)	15.4563(3)	13.0681(6)	11.9444(5)
b, Å	10.3501(2)	18.1151(3)	11.0392(3)	17.1733(4)	16.6740(4)	16.8690(7)
c, Å	18.4778(5)	26.8307(4)	16.3726(4)	19.0480(4)	14.3973(2)	18.639(07)
α, deg	90	90	90	72.245(1)	90	69.769(2)
β, deg	90.874(1)	90	110.568(1)	71.802(1)	91.298(1)	77.738(2)
γ, deg	90	90	90	78.565(1)	90	79.183(2)
V, Å^3	1075.89(5)	7161.8(2)	2669.5(1)	4544.60(17)	3136.3(2)	3416.7(2)
Z	4	8	4	4	4	2
$D_{calcd.}$, g cm^{-3}	1.37	1.18	1.50	1.30	1.32	1.29
μ(MoK_α), cm^{-1}	0.8	0.7	18.3	12.0	1.0	2.3
Refl. coll. / unique / R_{int}	6451 / 2458 / 0.028	35909 / 14586 / 0.050	16602 / 6106 / 0.024	29015 / 20187 / 0.022	18688 / 7157 / 0.034	20552 / 14674 / 0.035
Refl. with $I > 2\sigma(I)$	2120	10895	5488	16935	5763	11042
$R_1 [I > 2\sigma(I)]^a$	0.0427	0.0933	0.0261	0.0447	0.0631	0.0973
wR_2 (all data, on F^2)^a	0.0996	0.2685	0.0706	0.0998	0.1711	0.1827
GoF^b	1.055	1.072	0.937	1.072	1.043	1.280
x (Flack)	–	−0.3(19)	–	–	–	–
$\Delta\rho_{fin}$ (max / min), e Å^{-3}	0.21 / −0.21	1.05 / −0.48	0.35 / −0.32	0.79 / −0.69	0.69 / −0.84	0.52 / −0.44
CCDC No.	871915	871916	871917	872906	871918	871919

^{a} Definition of the R indices: $R_1 = \Sigma||F_o| - |F_c||/\Sigma|F_o|$; $wR_2 = [\Sigma w(F_o^2 - F_c^2)^2/\Sigma w(F_o^2)^2]^{1/2}$, $w = [\sigma^2(F_o^2) + (AP)^2 + BP]^{-1}$, where $P = (\text{Max}(F_o^2, 0) + 2F_c^2)/3$ and A and B are constants adjusted by the program; ^{b} GoF $= S = [\Sigma w(F_o^2 - F_c^2)^2/(n_{obs} - n_{param})]^{1/2}$, where n_{obs} is the number of data and n_{param} the number of refined parameters.

7.30 (t, $^3J(H^{33},H^{32,34})$ = 7.6 Hz, 2H, H^{33}), 7.11 (t, $^3J(H^{34},H^{33})$ = 7.4 Hz, 1H, H^{34}), 7.05 (s, 1H, H^4), 6.98 (t, $^3J(H^{54},H^{53,55})$ = 5.9 Hz, 1H, H^{54}). – ^{13}C NMR (400 MHz, 300 K, [D$_8$]thf): δ = 154.4 (C^3), 153.7 (C^{51}), 149.7 (C^5), 148.8 (C^{53}), 139.2 (C^{55}), 138.0 (C^{31}), 128.6 (C^{33}), 125.8 (C^{34}), 125.6 (C^{32}), 121.2 (C^{54}), 119.1 (C^{56}), 98.8 (C^4). – MS (EI): m/z (%) = 488* (12) [M+Mg–2thf/diox]$^+$, 464* (2) [M–2thf/diox]$^+$, 354 (16), 244* (20) [M–2thf/diox, ligand]$^+$, 221 (48) [ligand]$^+$, 192 (100) [ligand–N$_2$]$^+$. – IR (cm^{-1}): ν = 3076 vw, 3052 w, 2976 w, 2893 w, 2864 w, 1601 vs, 1560 s, 1527 s, 1457 s, 1441 vs, 1369 m, 1332 w, 1294 w, 1280 w, 1259 m, 1228 m, 1187 m, 1151 m, 1117 s, 1094 w, 1075 s, 1044 vs, 1017 m, 989 vs, 956 m, 916 m, 888 m, 873 vs, 802 s, 785 s, 765 vs, 753 s, 724 s, 698 s, 683 s, 644 s, 615 m, 527 w, 498 w, 465 s, 435 w, 417 s.

Synthesis of [{(thf)$_2$Ca}(μ-Pz)$_3$Ca(Pz)] (5)

2-(3-Phenyl-1H-pyrazol-5-yl)pyridine (500 mg, 2.26 mmol) was dissolved in 15 mL of thf. Potassium hydride (200 mg, 4.99 mmol) was added and the mixture stirred for 20 min. Excessive KH was removed and calcium diiodide (332 mg, 1.13 mmol) added. The reaction mixture was stirred over night and precipitated potassium iodide removed by filtration. 75 % of the solvent was removed and the solution stored at –20 °C. Colorless needles of the thf adduct **5** were obtained. Yield: 300 mg (1.15 mmol, 51 %). M. p. 342 °C. – ^{1}H NMR (400 MHz, 300 K, [D$_8$]thf/dmso): δ = 8.56 (s, 1H, H^{53}), 7.92 (d, $^3J(H^{32},H^{33})$ = 6.9 Hz, 2H, H^{32}), 7.86 (s, 1H, H^{56}), 7.66 (s, 1H, H^{55}), 7.29 (s, 2H, H^{33}), 7.09–7.05 (m, 2H, $H^{4,34}$), 6.96 (s, 1H, H^{54}). – ^{13}C NMR (400 MHz, 300 K, [D$_8$]thf/dmso): δ = 155.6 (C^{51}), 151.9 ($C^{3,5}$), 150.2 (C^{53}), 138.2 (C^{31}), 137.7 (C^{55}), 128.9 (C^{33}), 125.7 ($C^{32,34}$), 120.4 (C^{54}), 119.8 (C^{56}), 100.2 (C^4). – MS (EI): m/z (%) = 479* (2) [M–thf, H]$^+$, 402* (2) [M–thf, PhH]$^+$, 316 (36), 260* (100) [M–thf, ligand]$^+$, 221 (85) [ligand]$^+$, 192 (76) [ligand–N$_2$]$^+$. – IR (cm^{-1}): ν = 3062 w, 2973 w, 2956 w, 2882 vw, 2853 w, 1597 vs, 1564 m, 1527 m, 1455 m, 1439 vs, 1381 w, 1330 w, 1277 w, 1253 w, 1226 m, 1152 m, 1119 m, 1103 w, 1073 m, 1053 s, 1032 m, 1006 m, 982 vs, 910 m, 888 m, 873 s, 780 s, 755 vs, 721 vs, 697 vs, 684 vs, 631 s, 531 m, 521 w, 493 vw, 432 m, 414 vs, 405 vs.

Structure determinations

The intensity data for the compounds were collected on a Nonius KappaCCD diffractometer, using graphite-monochromatized MoK_α radiation (λ = 0.71073 Å). Data were corrected for Lorentz and polarization effects but not for absorption [56, 57]. The structures were solved by Direct Methods (SHELXS [58]) and refined by full-matrix least-squares techniques against F^2 (SHELXL-97 [58]). All hydrogen atoms of compound **1** were located by difference Fourier techniques and refined isotropically. All other hydrogen atoms were included in calculated positions with fixed thermal parameters. All non-disordered, non-hydrogen atoms were refined anisotropically [58]. Crystallographic data as well as structure solution and refinement details are summarized in Table 3. XP (Siemens Analytical X-ray Instruments, Inc.) was used for structure representations.

CCDC 871915 (**1**), 871916 (**2**), 871917 (**3a**), 872906 (**3b**), 871918 (**4**), and 871919 (**5**) contain the supplementary crystallographic data for this paper. These data can be obtained free of charge from The Cambridge Crystallographic Data Centre *via* www.ccdc.cam.ac.uk/data_request/cif.

[1] F. T. Edelmann, *Adv. Organomet. Chem.* **2008**, *57*, 183 – 352.

[2] a) S. Trofimenko, *Chem. Rev.* **1972**, *72*, 497 – 509; b) S. Trofimenko, *Chem. Rev.* **1993**, *93*, 943 – 980.

[3] E. C. Constable, P. J. Steel, *Coord. Chem. Rev.* **1989**, *93*, 205 – 223.

[4] E. Bouwman, W. L. Driessen, J. Reedijk, *Coord. Chem. Rev.* **1990**, *104*, 143 – 172.

[5] F. Mani, *Coord. Chem. Rev.* **1992**, *120*, 325 – 359.

[6] R. Mukherjee, *Coord. Chem. Rev.* **2000**, *203*, 151 – 218.

[7] a) C. Pettinari, R. Pettinari, *Coord. Chem. Rev.* **2005**, *249*, 525 – 543; b) C. Pettinari, R. Pettinari, *Coord. Chem. Rev.* **2005**, *249*, 663 – 691.

[8] A. Torvisco, A. Y. O'Brien, K. Ruhlandt-Senge, *Coord. Chem. Rev.* **2011**, *255*, 1268 – 1292.

[9] V. Montoya, J. Pons, V. Branchadell, J. Ros, *Tetrahedron* **2005**, *61*, 12377 – 12385.

[10] W. R. Thiel, J. Eppinger, *Chem. Eur. J.* **1997**, *3*, 696 – 705. See also: W.-S. Yu, C.-C. Cheng, Y.-M. Cheng, P.-C. Wu, Y.-H. Song, Y. Chi, P.-T. Chou, *J. Am. Chem. Soc.* **2003**, *125*, 10800 – 10801.

[11] A. Chadghan, J. Pons, A. Caubet, J. Casabó, J. Ros, A. Alvarez-Larena, J. F. Piniella, *Polyhedron* **2000**, *19*, 855 – 862.

[12] J. Pons, A. Chadghan, A. Alvarez-Larena, J. F. Piniella, J. Ros, *Inorg. Chim. Acta* **2001**, *324*, 342 – 346.

[13] J. Pons, A. Chadghan, J. Casabó, A. Alvarez-Larena, J. F. Piniella, X. Solans, M. Font-Bardia, J. Ros, *Polyhedron* **2001**, *20*, 1029 – 1035.

[14] J. Pons, A. Chadghan, J. Casabó, A. Alvarez-Larena, J. F. Piniella, J. Ros, *Polyhedron* **2001**, 2531 – 2536.

[15] J. Benet-Buchholz, P. Comba, A. Llobet, S. Roeser, P. Vadivelu, S. Wiesner, *Dalton Trans.* **2010**, *39*, 3315 – 3320.

[16] Y. Kashiwame, M. Watanabe, K. Araki, S. Kuwata, T. Ikariya, *Bull. Chem. Soc. Jpn.* **2011**, *84*, 251 – 258.

[17] V. Montoya, J. Pons, J. García-Antón, X. Solans, M. Font-Bardía, J. Ros, *Organometallics* **2007**, *26*, 3183 – 3190.

[18] J. Pons, A. Chadghan, J. Casabó, A. Alvarez-Larena, J. F. Piniella, J. Ros, *Inorg. Chem. Commun.* **2000**, *3*, 296 – 299.

[19] J. A. Perez, J. Pons, X. Solans, M. Font-Bardía, J. Ros, *Inorg. Chim. Acta* **2005**, *358*, 617 – 622.

[20] G. Gupta, C. Zheng, P. Wang, K. M. Rao, *Z. Anorg. Allg. Chem.* **2010**, *636*, 758 – 764.

[21] B. Zhao, H.-M. Shu, H.-M. Hu, T. Qin, X.-L. Chen, *J. Coord. Chem.* **2009**, *62*, 1025 – 1034.

[22] H. Hennig, *J. Prakt. Chem.* **1966**, *34*, 64 – 68.

[23] M. Westerhausen, M. Wieneke, H. Nöth, T. Seifert, A. Pfitzner, W. Schwarz, O. Schwarz, J. Weidlein, *Eur. J. Inorg. Chem.* **1998**, 1175 – 1182.

[24] M. F. Lappert, P. P. Power, A. R. Sanger, R. C. Srivastava, *Metal and Metaloid Amides: Syntheses, Structures, and Physical and Chemical Properties*, Ellis Horwood, Chichester; **1980**, chapter 2, p. 24 – 44.

[25] W. N. Setzer, P. v. R. Schleyer, *Adv. Organomet. Chem.* **1985**, *24*, 353 – 451.

[26] K. Gregory, P. v. R. Schleyer, R. Snaith, *Adv. Inorg. Chem.* **1991**, *37*, 47 – 142.

[27] R. E. Mulvey, *Chem. Soc. Rev.* **1991**, *20*, 167 – 209.

[28] F. Pauer, P. P. Power in *Lithium Chemistry: A Theoretical and Experimental Overview*, (Eds.: A. M. Sapsa, P. v. R. Schleyer); Wiley, New York; **1995**, chapter 9, pp. 295 – 392.

[29] M. Lappert, A. Protchenko, P. Power, A. Seeber, *Metal Amide Chemistry*, Wiley, Chichester; **2009**, chapter 2, pp. 7 – 38.

[30] L. M. Engelhardt, G. E. Jacobsen, P. C. Junk, C. L. Raston, B. W. Skelton, A. H. White, *J. Chem. Soc., Dalton Trans.* **1988**, 1011 – 1020.

[31] C. Jones, P. C. Junk, N. A. Smithies, *J. Organomet. Chem.* **2000**, *607*, 105 – 111.

[32] M. Westerhausen, A. N. Kneifel, N. Makropoulos, *Inorg. Chem. Commun.* **2004**, *7*, 990 – 993.

[33] M. Westerhausen, A. N. Kneifel, P. Mayer, H. Nöth, *Z. Anorg. Allg. Chem.* **2004**, *630*, 2013 – 2021.

[34] M. Westerhausen, A. N. Kneifel, P. Mayer, *Z. Anorg. Allg. Chem.* **2006**, *632*, 634 – 638.

[35] C. Koch, H. Görls, M. Westerhausen, *Acta Crystallogr.* **2007**, *E63*, m2633 – m2634.

[36] J. Weston, *Chem. Rev.* **2005**, *105*, 2151 – 2174.

[37] F. Meyer, *Eur. J. Inorg. Chem.* **2006**, 3789 – 3800.

[38] J. Klingele, S. Dechert, F. Meyer, *Coord. Chem. Rev.* **2009**, *253*, 2698 – 2741.

[39] M. Melnik, J. Skoršepa, K. Györyová, C. E. Holloway, *J. Organomet. Chem.* **1995**, *503*, 1 – 9.

[40] T. Kloubert, H. Görls, M. Westerhausen, *Z. Anorg. Allg. Chem.* **2010**, *636*, 2405 – 2408.

[41] M. Westerhausen, T. Bollwein, N. Makropoulos, T. M. Rotter, T. Habereder, M. Suter, H. Nöth, *Eur. J. Inorg. Chem.* **2001**, 851 – 857.

[42] C. Koch, H. Görls, M. Westerhausen, *Acta Crystallogr.* **2007**, *E63*, m2732.

[43] A. Malassa, C. Koch, B. Stein-Schaller, H. Görls, M. Friedrich, M. Westerhausen, *Inorg. Chim. Acta* **2008**, *361*, 1405 – 1414.

[44] C. Koch, H. Görls, M. Westerhausen, *Acta Crystallogr.* **2008**, *E64*, m664.

[45] L. M. Engelhardt, P. C. Junk, W. C. Patalinghug, R. E. Sue, C. L. Raston, B. W. Skelton, A. H. White, *J. Chem. Soc., Chem. Commun.* **1991**, 930 – 932.

[46] M. Westerhausen, T. Bollwein, N. Makropoulos, S. Schneiderbauer, M. Suter, H. Nöth, P. Mayer, H. Piotrowski, K. Polborn, A. Pfitzner, *Eur. J. Inorg. Chem.* **2002**, 389 – 404.

[47] C. Koch, A. Malassa, C. Agthe, H. Görls, R. Biedermann, H. Krautscheid, M. Westerhausen, *Z. Anorg. Allg. Chem.* **2007**, *633*, 375 – 382.

[48] M. G. Cushion, J. Meyer, A. Heath, A. D. Schwarz, I. Fernández, F. Breher, P. Mountford, *Organometallics* **2010**, *29*, 1174 – 1190.

[49] M. Westerhausen, *Trends Organomet. Chem.* **1997**, *2*, 89 – 105.

[50] M. Westerhausen, *Coord. Chem. Rev.* **1998**, *176*, 157 – 210.

[51] M. Gärtner, H. Görls, M. Westerhausen, *Inorg. Chem.* **2007**, *46*, 7678 – 7683.

[52] M. Gärtner, H. Görls, M. Westerhausen, *Dalton Trans.* **2008**, 1574 – 1582.

[53] C. Glock, H. Görls, M. Westerhausen, *Inorg. Chem.* **2009**, *48*, 394 – 399.

[54] C. Glock, H. Görls, M. Westerhausen, *Inorg. Chim. Acta* **2011**, *374*, 429 – 434.

[55] C. Glock, H. Görls, M. Westerhausen, *Dalton Trans.* **2011**, *40*, 8108 – 8113.

[56] R. Hooft, COLLECT, Nonius KappaCCD Data Collection Software, Nonius BV, Delft (The Netherlands) **1998**.

[57] Z. Otwinowski, W. Minor in *Methods in Enzymology*, Vol. 276, *Macromolecular Crystallography*, Part A (Eds.: C. W. Carter Jr, R. M. Sweet), Academic Press, New York, **1997**, pp. 307 – 326.

[58] G. M. Sheldrick, SHELXS/L-97, Programs for Crystal Structure Determination, University of Göttingen, Göttingen (Germany) **1997**. See also: G. M. Sheldrick, *Acta Crystallogr.* **1990**, *A46*, 467 – 473; *ibid.* **2008**, *A64*, 112 – 122.